SEAL RELIABILITY AND PERFORMANCE IMPROVEMENTS IN A LARGE, HIGH-PRESSURE, HIGH-TEMPERATURE BARREL PUMP

by
Ed Wilcox
Senior Staff Engineer
Conoco, Inc.
Westlake, Louisiana

Ed Wilcox is a Senior Staff Engineer with Conoco, Inc., in Westlake, Louisiana, where he is the Reliability Engineer for Excel-Paralubes, a joint venture between Conoco and Pennzoil. He also provides technical support for the adjacent Conoco Refinery. His responsibilities include maintenance, troubleshooting, and specification of rotating equipment.

Mr. Wilcox received his BSME degree from the University of Missouri-Rolla and MSME degree from Oklahoma State University. He has also done post graduate work at the Georgia Institute of Technology in the areas of machinery vibration, lubrication, and rotordynamics. He is a Vibration Institute certified Level III Vibration Specialist, a member of STLE, and a registered Professional Engineer in the State of Oklahoma.

ABSTRACT

Modifications to a high-pressure, high-temperature barrel pump to increase seal reliability and throughput are discussed. The pump is in unspared hydrodewaxer (HDW) feed service. The original seal design included nonpressurized dual seals to provide an additional level of reliability. However, due to the heavy-oil/high-temperature nature of the service, the dual seals produced less than desirable run times. Substantial modifications to the dual seals were made to improve their reliability, but this also proved to be disappointing. Finally, the dual seals were replaced with single seals of a different design resulting in much more favorable results. The paper provides a detailed description of both seal modifications and their results. After approximately two years of service the capacity of the pump became the unit limit. The throughput of the pump was increased by approximately 25 percent without substantial capital outlays. This performance increase was accomplished by modifying the impeller diameter, the impeller vane tip widths, and reducing the internal circulation through the use of high temperature abraidable materials and reduced internal clearances. These modifications were preceded by a rotordynamic analysis of the pump before and after the internal clearances were reduced. Performance and vibration data before and after the modifications are presented.

SUMMARY

This paper describes the modifications made to a large high-pressure barrel pump to increase its reliability and throughput. A detailed description of the seal problems and the progressive modifications are given. Likewise, the methods used to increase the capacity of the pump with minimal capital expense are given. A description of the rotordynamic analysis performed for these modifications is also given.

ORIGINAL DESIGN

The pump is in nonspared charge service for a hydrodewaxer (HDW) unit in a Gulf Coast refinery/lube plant. The pump is a 13-stage, high-pressure, high-temperature barrel design that pumps heavy gas oil from 40 psig to approximately 4000 psig at a temperature of 500°F. The pump operates at 3550 rpm and is driven by a 3500 hp induction motor (Figure 1). The pump is a back-to-back impeller design with a seal equalizing line that results in both seal chamber pressures being approximately equal to suction pressure (Figure 2).

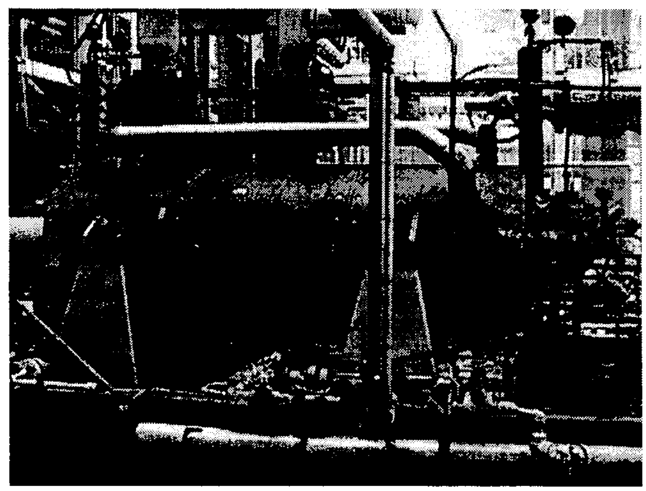

Figure 1. High-Pressure Barrel Pump.

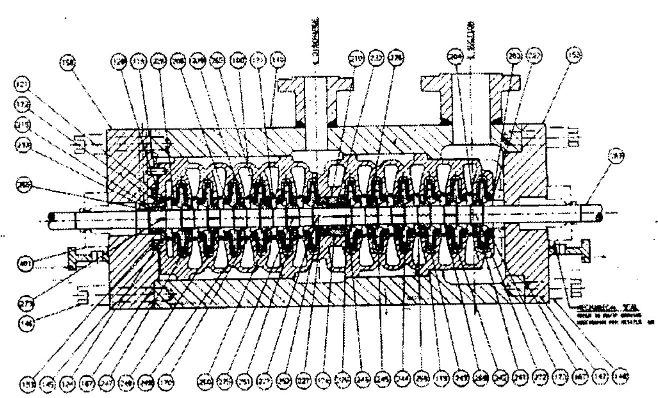

Figure 2. Cross-Section of High-Pressure Barrel Pump.

Because the pump is nonspared, the original design was nonpressurized dual seals to allow the pump to operate for an extended time on the secondary seal if the primary failed. The design incorporated tandem, rotating metal bellows seals with silicon-carbide versus carbon faces, and graphoil gaskets (Figure 3). A radial pumping ring (Figure 3, item 90) circulates oil from between the seals and the seal oil pot (API Plan 52). ISO 32 turbine oil was used as a barrier fluid. The seal sleeve under the rotating bellows was releaved to improve circulation of the barrier fluid. The seal oil pot was vented to the flare through a 1/8 inch restriction orifice.

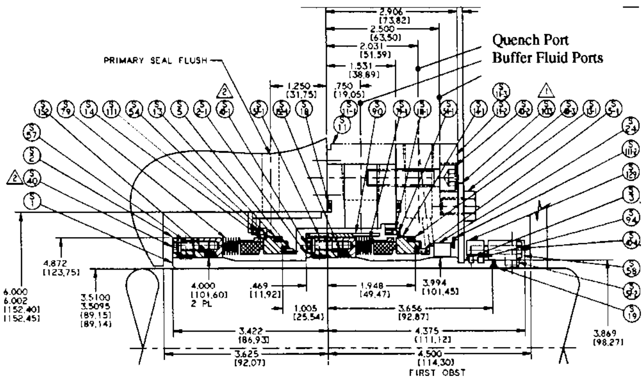

Figure 3. Dual Seal with Rotating Metal Bellows, Original Design.

SECONDARY SEAL PROBLEMS

Approximately one month after startup of the HDW unit, the pump began experiencing secondary seal problems. Barrier fluid began dripping from the seal and had to be continually added to the seal oil pot. Because the seal was a tandem design, there was not enough axial space for an anti-coking device on the atmospheric side of the secondary seal (Figure 3). A steam lance was applied to the exterior of the seal close to the seal gland and it reduced the leakage rate. Likewise, over time the heavy/waxy gas oil from the process began to slowly collect in the seal oil pot and leak out the secondary seal (Figures 4 and 5). The fog of gas oil created by the leaking seal caused waxy oil to accumulate in the bearing housing and contaminated the lube oil system. The 3/4 inch tubing lines from the seal glands and seal pots became completely plugged off with wax. The plugging problem was complicated by the seal oil pot excessive temperature. Even though the pot had a 1/2 inch cooling coil, the exterior temperature was approximately 240 to 250°F.

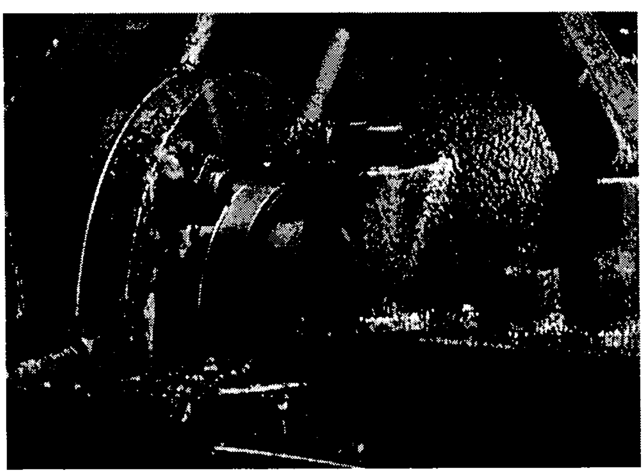

Figure 4. Waxy Oil Leaking from Secondary Seal.

FIRST MODIFICATION

Pressurized Tandem

Approximately one year after the pump was commissioned, the primary seal on one end of the pump began leaking excessively.

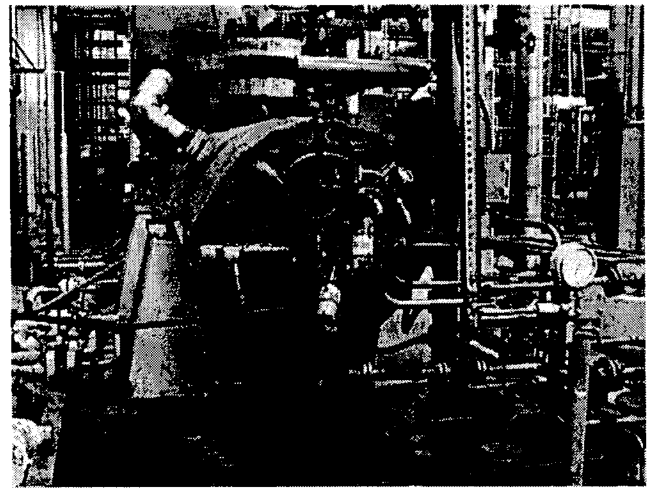

Figure 5. Oil Vapor Blowing Out of Secondary Seal and Accumulating on Baseplate.

This caused the seal pot to pressure up to approximately 30 psig, which blew out the secondary seal. Inspection of the seal revealed a large amount of coking on the outside of the secondary seal and excessive wear on the secondary seal faces (Figures 6 and 7).

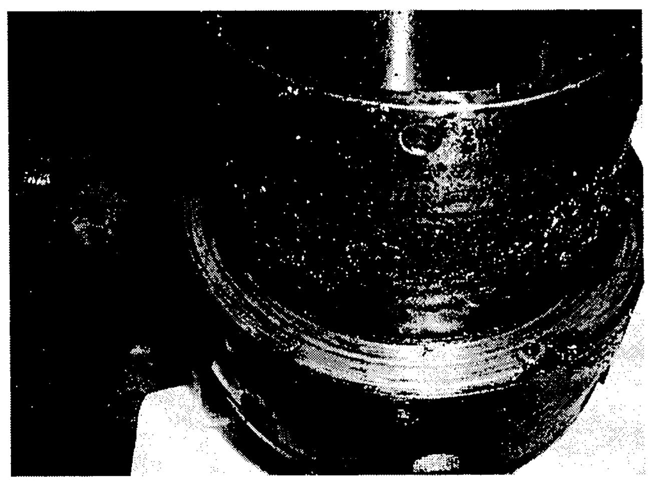

Figure 6. Wax and Coke Buildup Under Primary Bellows (Back of Secondary Seal).

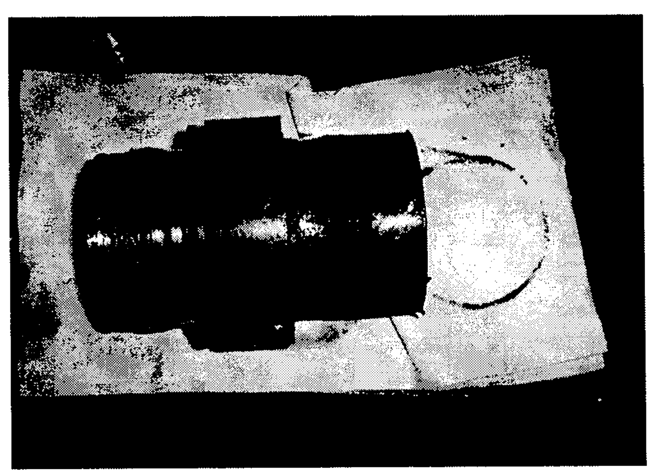

Figure 7. Coke Buildup on Sleeve (Secondary Seal Is Still on the Sleeve).

It was thought that the waxy gas oil was eventually contaminating the seal oil pot to the point that the secondary seal was running dry, which resulted in the excessive face wear. Likewise, because of the high surface velocity and low fluid pressure on the secondary seal (1 psig), it was thought that the secondary seal was not being properly lubricated (i.e., the centrifugal effects on the oil were overcoming the hydrodynamic pumping action of the seal). This was confirmed by the evidence on the secondary seal carbon face that the seal was running hot and contacting on the inside diameter (Figures 8 and 9). A hydrodynamic/thermal model (Lebeck, 1991) of the seal faces confirmed that there was a large amount of thermal deflection of the rotating seal face. This produces a highly convergent face profile resulting in contact on the inside diameter of the seal faces (Figure 10).

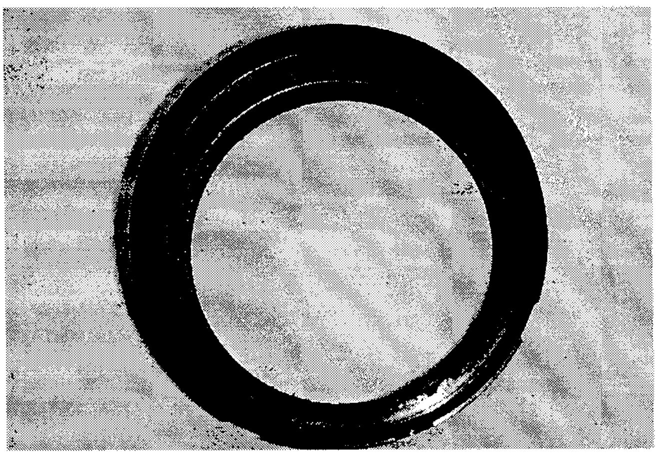

Figure 8. Secondary Seal Face Showing Evidence of Excessive Heat/Lack of Lubrication.

Figure 9. Closeup of Secondary Seal Face Showing Evidence of Dry Running on Inside Diameter.

One solution considered was using a slight nitrogen purge to raise the seal pot pressure to approximately 20 psig. This had been done on other applications where lubrication of the secondary seal had been a problem. However, this solution was not implemented because it would not eliminate the problems associated with the waxy process oil accumulating in the seal pot. Likewise, it was thought that if the waxy buildup in the seal pots caused the secondary to fail, the added pressure would cause the secondary seals to leak even more.

The seal design was changed to a pressurized tandem. This would keep the waxy gas oil out of the seal pot and also provide

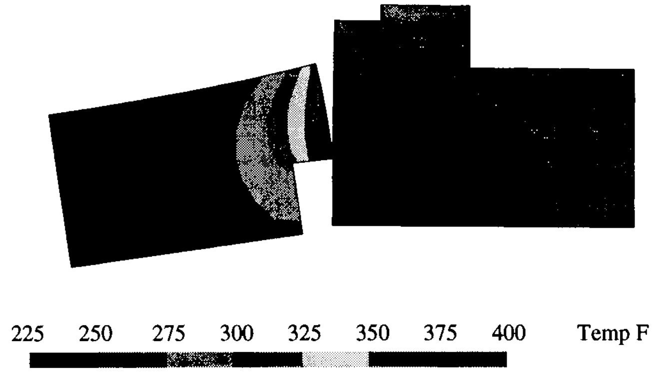

Figure 10. Predicted Temperature Profiles in Secondary Seal Faces Showing Convergent Profile.

adequate lubrication to the secondary seal. The seal pot was pressurized to approximately 20 psid above the stuffing-box pressure using nitrogen. A low level alarm was installed on each pot (Figure 11). Buffer fluid was added to the seal pots using an injection pump. Even though an anti-coking device was not available due to limited axial space, a steam quench was installed to the quench port shown in Figure 3. This was an improvement over the steam lance directed at the outside of the seal. However, the carbon bushing (Figure 3, item 24) did little to force the steam up under the bellows.

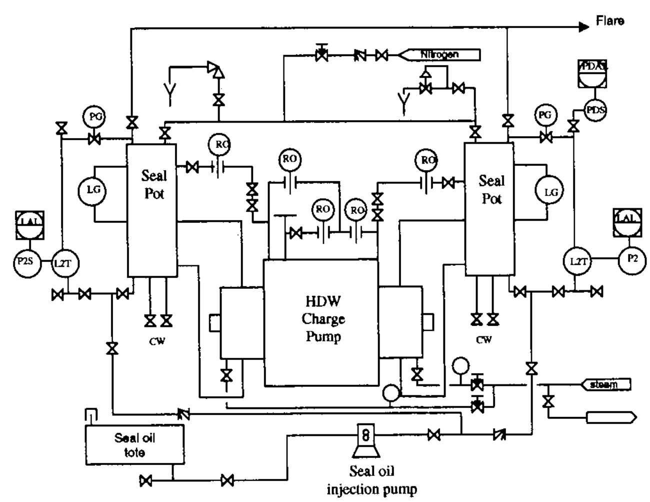

Figure 11. Schematic of Pressurized Seal Oil System.

By this time the seal oil system had become quite complicated (Figures 11 and 12). Each seal pot had a local level indicator that activated a common alarm in the control room if the level dropped too low. Likewise, there was a differential pressure switch that monitored the differential pressure between the seal pot and the pump stuffing-box. It was also tied into the common trouble alarm. A nitrogen pressure regulator was used to maintain the seal oil differential pressure. Also, a relief valve had to be added to the system to protect the seal pot from a blocked in liquid scenario.

The pressurized tandem configuration eliminated the problem with waxy oil accumulating in the seal oil pots. Likewise, it improved the lubrication of the secondary seal (i.e., the secondary seal faces showed no evidence of dry running) (Figure 13). However, after a few months of operation, leakage from the seal oil pot began increasing to the point where operations personnel were required to fill the pot once every two hours (approximately 1 gal/hour per seal). Most of the leakage was past the primary seal into the pump, though the secondary seal continued to be plagued

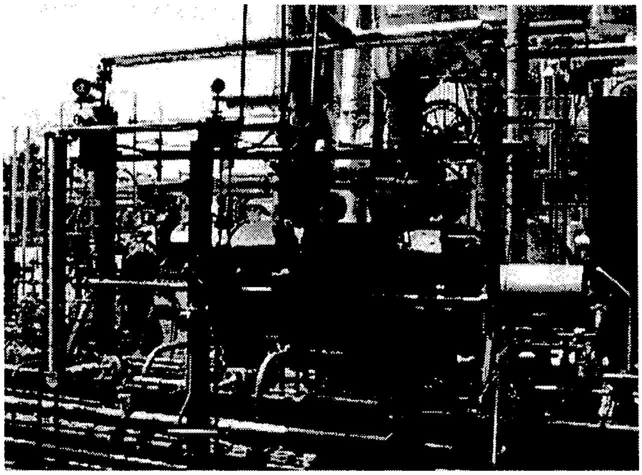

Figure 12. Pressurized Seal Oil System.

by an occasional drip as well. Reducing the differential pressure to 10 and then 5 psid reduced the leakage rate somewhat; however, it was still very difficult to maintain.

Figure 13. Secondary Seal Face After Two Years of Operation (Pressurized).

SECOND MODIFICATION

Primary Seal Balance Change

Both primary and secondary seals were originally designed with a 60 percent OD balance and a 40 percent ID balance. Approximately nine months after the seals on the HDW pump were converted to pressurized tandems, the HDW unit was brought down for a catalyst change. At this time, to reduce the leakage past the primary seal, it was modified to give it a 60 percent ID balance. Obviously, this would increase the seal face loading of the inner seal when it was pressurized from the ID.

These modifications did not improve the seal oil leakage rates. After approximately one month, the leakage rate into the pump became unmanageable. Operations was having to add oil to the seal pots every hour. An alternate external flushing source was located and the seal oil pot was modified so that the external flush oil entered the bottom and exited the top before entering the pump stuffing-box through a restriction orifice (Figure 14). The seal pots were liquid full at all times; however, there was a continuous flow through the pots from bottom to top. This eliminated the need to fill the pot every hour and lowered the seal oil pot temperature to approximately 140°F. Likewise, nitrogen was no longer required to pressurize the pots.

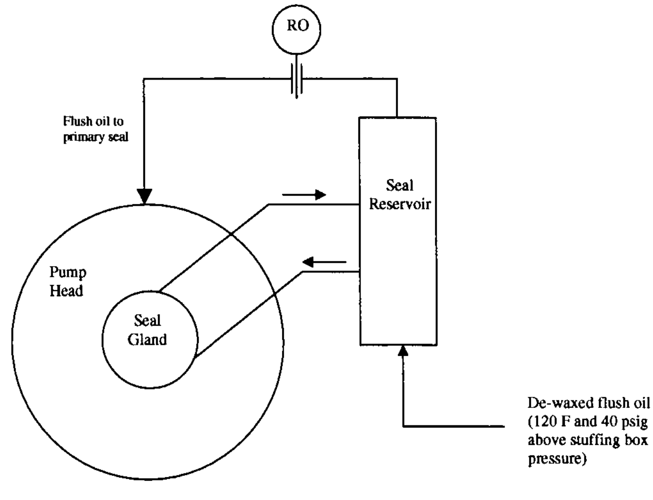

Figure 14. External Flush Used to Supply Seal Oil Pot (API Plan 32/53).

THIRD MODIFICATION

Change to Single Seals

Several different factors contributed to the dual seals lack of reliability:

- As mentioned above, an anti-coking device was not available on the secondary seal due to axial space limitations. A steam quench was applied through the quench port; however, this still did not provide enough steam to the seal faces to keep them free of waxy buildup.
- A rotating bellows was used because there was not enough axial space for two stationary bellows. Because of the large seal diameter, the surface velocity (70 fps) was close to the maximum for the seal (75 fps). This may have contributed to its instability.
- Leakage from the seal pot into the pump (i.e., past the primary seal) may have been a result of poor fluid circulation under the primary bellows (even though the seal sleeve was relieved under the bellows), which could have caused excessive temperature. This was supported by the large amount of coking found under the primary bellows. Because of the tandem arrangement, there is only a 0.125 inch clearance between the back of the primary seal and the front of the secondary seal (Figure 3).
- Nonpressurized tandems are normally used on light hydrocarbon or hazardous applications such as propane, naphtha, or sour water. These process fluids would normally vaporize in the seal pot and be vented to flare. The heavy gas oil would not vaporize, but collected in the seal pot. Likewise, when the primary seal leaked excessively and filled up the seal pot, it would fill the flare line with heavy oil that partially blocked it off and caused a safety hazard.

Adding the continuous flush to the seal pot improved the reliability of the seals. However, these seals did not provide the additional backup that the seals were originally designed for, i.e., if either seal failed, the pump would be down. Therefore, the pump's susceptibility to failure was twice as high because if only one of four seals failed, the pump would have to be shut down.

A single, stationary metal bellows seal was selected to replace the dual seals (Figure 15). Because more axial space was available with a single seal, an anti-coking device could be incorporated in the design and a thicker bellows was used. Likewise, the seal flush that had been used to fill the seal pots was now used as an external flush on the seals, i.e., API Plan 32. The seal flush was routed through the seal gland instead of the gland tap to ensure adequate flow past the seal faces. Likewise, the Plan 11 flush from the discharge was blocked in. Because of its stationary bellows design and more rugged construction, the single seal had a much higher speed rating of 125 fps.

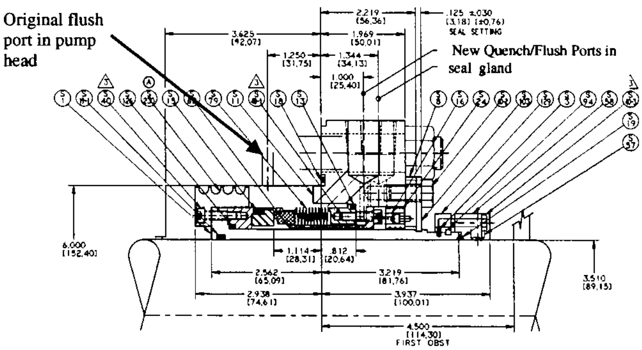

Figure 15. Single, Stationary Metal Bellows Seal.

RESULTS OF SEAL MODIFICATIONS

The single seals were installed during the first major turnaround of the HDW unit. The new seals have operated a year with no problems.

PERFORMANCE UPGRADES

After two years of operation, various process bottlenecks had been eliminated in the HDW unit such that the charge pump had become the unit limit. The HDW charge pump needed a 25 percent increase in capacity, but very little increase in head. The modifications had to be made within six weeks to meet a catalyst change window. The capacity increase was accomplished with the following modifications:

• *Increase impeller diameter*—The new process conditions required were 9500 ft at 1060 gpm. Increasing the impeller size to the maximum diameter allowed by API would only produce 8300 ft at 1060 gpm (Figure 16). The API maximum impeller diameter is set by the requirement that the minimum gap between the impeller vane and volute tip be 6 percent of the impeller diameter. Because this was substantially below the required conditions, it was decided to increase the impeller diameter to 14.00 inches, which gives a volute to vane tip clearance of 3.5 percent. However, this was still short of the desired performance (Figure 16).

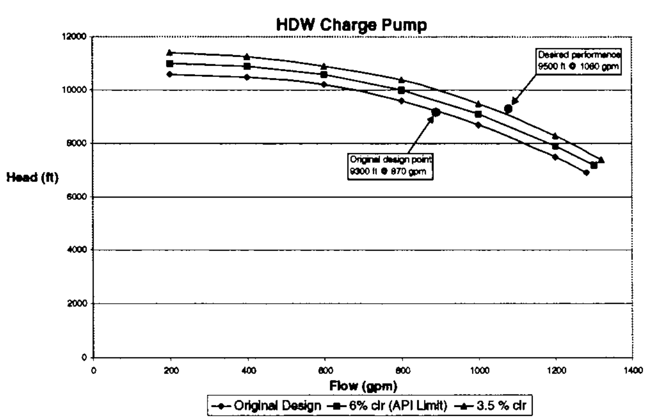

Figure 16. Original Performance, Performance with 6 Percent CLR, and 3.5 Percent CLR.

• *Impeller underfiling*—Underfiling the impeller vanes shifts the head curve to the right (Figure 17). This is accomplished by modifying the exit velocity triangle of the pump. Illustrations of the theoretical inlet and exit velocity triangles are given in Figure 18. The actual velocity triangles vary from those shown in Figure 18 due to deviation of the fluid from the vane angle, i.e., slip. The slip factor, μ, is used to calculate the actual peripheral exit velocity, c'_{u2}, from the idealized value, c_{u2} (Equation (1) (Karassik, et al., 1986)).

$$\mu = \frac{c'_{u2}}{c_{u2}} \tag{1}$$

Likewise, the slip factor is assumed to be a function of the number of impeller vanes and vane angle (Equation (2) (Karassik, et al., 1986)).

$$\mu = 1 - \frac{\pi \sin(\beta_2)}{z} \tag{2}$$

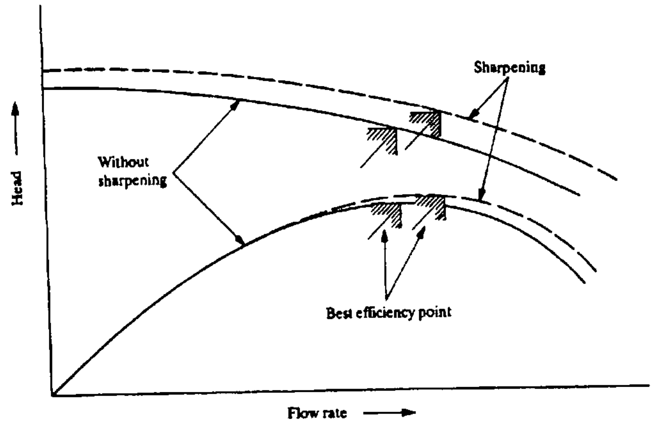

Figure 17. Effects of Vane Underfiling on Performance Curve.

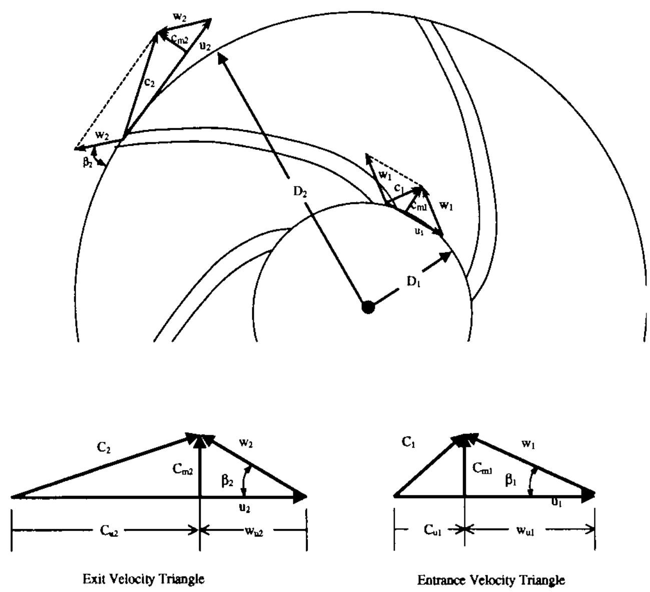

Figure 18. Inlet and Exit Velocity Triangles for Centrifugal Pump.

Underfiling the vanes increases the exit area, which lowers the average exit meridian velocity, c_{m2}. This in turn increases the value of the exit tangential velocity, c_{u2}, which increases the head produced at the same given flowrate. Likewise, the exit angle, β_2, is increased slightly, which also increases the head. These effects can be seen in Equation (3), which gives the formula for head produced by a centrifugal pump, assuming the inlet velocity is negligible.

$$H = \mu \frac{u_2^2}{g}\left(1 - \frac{c_{m2}}{u_2 * \tan \beta_2}\right) \tag{3}$$

Figures 19 and 20 show the effects underfiling has on the pump discharge velocity triangle. The vectors labeled with an "F" subscript are the result of underfiling. Figure 19 illustrates the increase in head at the same capacity, while Figure 20 shows the increase in capacity for the same given head.

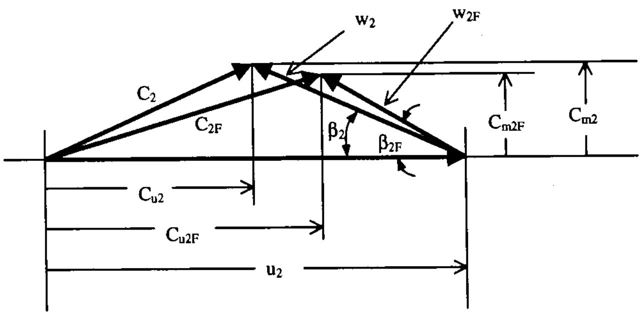

Figure 19. Increase in Head Due to Underfiling.

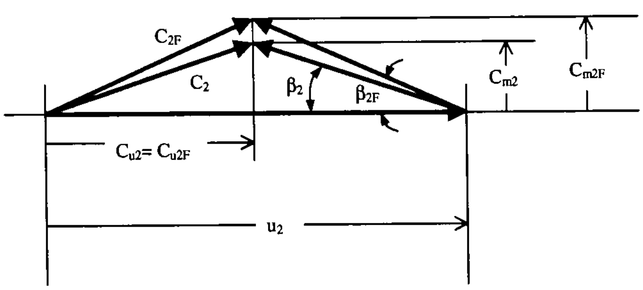

Figure 20. Increase in Capacity Due to Underfiling.

The impeller vane thickness at the tip was reduced from 13/16 inch to 3/16 inch (Figures 21, 22, and 23). This reduced the exit area in the impeller by approximately 3 to 4 percent. It was estimated that the underfiling would increase the capacity of the pump by at least 2 percent. Underfiling the vanes has the added benefit of reducing the pulsation produced by the vanes as they pass by the volute tip. This was especially a concern since the volute to vane tip clearance had been reduced as mentioned above. Angle cutting the impeller vanes and volute tips to reduce the pulsation was considered; however, it was not performed because it might have reduced the performance of the pump. It was believed that the other changes would reduce the pulsation to an acceptable level.

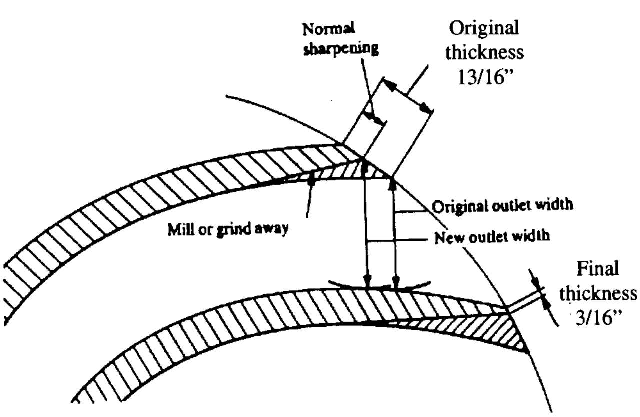

Figure 21. Underfiling Vanes.

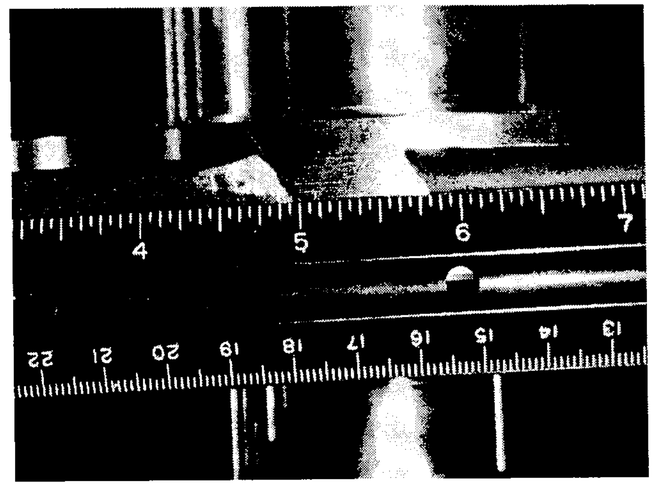

Figure 22. Impeller Vane Before Underfiling.

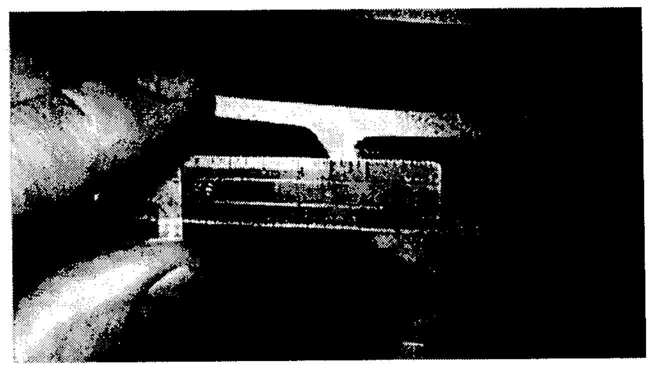

Figure 23. Impeller Vane After Underfiling.

• *Reduced clearance bushings*—The design temperature of the HDW charge pump was 500°F, which is the breakpoint between API standard and hot wear clearances. The clearances throughout the pump were originally specified as API standard, which corresponds to the OEMs hot clearances. To increase the capacity of the pump further, the diametral clearance of the center and throttle bushings (Figure 2, items 210 and 215) were reduced from 0.014 to 0.008 inch. Both of these bushings have a differential of approximately 1800 to 2000 psig. This reduced the estimated leakage through each bushing by 50 percent. Figures 24 and 25 show calculated leakage results. This resulted in a predicted increase in the capacity of approximately 3 to 4 percent. Additionally, it was hoped the lower clearance bushings would stabilize the rotor (i.e., increase support damping), which had been a concern because of the increase to maximum impeller diameter. A high-temperature graphite nickel material was used for the bushing because it would allow touching off without galling. Normally, this type of material would not be considered reliable in gas oil service due to its susceptibility to erosion. However, the gas oil was filtered through a 100 micron filter upstream of the pump to protect the HDW catalyst.

ROTORDYNAMIC ANALYSIS

Because of the lower vane-to-volute clearance and reduced clearance bushings, a rotordynamics analysis was conducted by the user to determine the effect these changes would have on the natural frequencies of the pump. The original OEM lateral analysis showed that the pump operated below its first critical (Figure 26). The user stability analysis showed that even though the first critical speed (as defined by API) was above the operating speed of the pump, the first eigenvalue (or natural mode) was actually below operating speed (Figure 27). Even though the damping factor (ξ) of

```
* p12001 center bushing
* 0.0014 clearance
*
* Units (0-in,1-m,2-mm) =          0   Output Format    (0-S,1-L) =        1
* Inlet Rad. Clr.   (in) =      0.007  Rotor Speed          (rpm) =     3550
* Exit Rad. Clr.    (in) =      0.007  Inlet Tang. Vel. Ratio (-) =      0.5
* Shaft Diameter    (in) =       4.87  Inlet Loss Factor      (-) =      0.3
* Seal Length       (in) =          3  Inlet Pressure       (psi) =     4000
* Rotor Rel. Rghns. (-) =           0  Exit Pressure        (psi) =     2000
* Stator Rel. Rghns.(-) =           0  Cavitation Pressure  (psi) =        5
* Ecc. X-Axis        (-) =        0.1  Inlet Visc.   (lbm/(ft-s)) =   0.0005
* Ecc. Y-Axis        (-) =        0.1  Inlet Density    (lbm/ft3) =       50
*
* STEADY-STATE SOLUTION
* Mass flow Rate           (lbm/s)=      8.486
* Volumetric flow Rate       (GPM)=      76.18
* Axial Reynold's Number      (--)=  2.662e+04
* Load Supported             (lbf)=      586.3
* Calc. Reaction Load Ang.   (deg)=  -155.8355
```

Figure 24. Leakage Through Center Bushing, Original OEM Clearance.

```
* P-12001 Center bushing
* 0.008 clr
*
* Units (0-in,1-m,2-mm) =          0   Output Format    (0-S,1-L) =        1
* Inlet Rad. Clr.   (in) =      0.004  Rotor Speed          (rpm) =     3550
* Exit Rad. Clr.    (in) =      0.004  Inlet Tang. Vel. Ratio (-) =      0.5
* Shaft Diameter    (in) =       4.87  Inlet Loss Factor      (-) =      0.3
* Seal Length       (in) =          3  Inlet Pressure       (psi) =     4000
* Rotor Rel. Rghns. (-) =           0  Exit Pressure        (psi) =     2000
* Stator Rel. Rghns.(-) =           0  Cavitation Pressure  (psi) =        5
* Ecc. X-Axis        (-) =        0.1  Inlet Visc.   (lbm/(ft-s)) =   0.0005
* Ecc. Y-Axis        (-) =        0.1  Inlet Density    (lbm/ft3) =       50
*
* STEADY-STATE SOLUTION
* Mass flow Rate           (lbm/s)=      3.339
* Volumetric flow Rate       (GPM)=      29.98
* Axial Reynold's Number      (--)=  1.048e+04
* Load Supported             (lbf)=      406.2
* Calc. Reaction Load Ang.   (deg)=  -174.2514
```

Figure 25. Leakage Through Center Bushing, Reduced Clearance.

the first mode is lower than that of the second mode, it does not produce a resonance peak in the forced response plot (Figure 28), due to the large amount of damping provided by the journal bearings. The second lateral mode shape, with the original OEM clearances, is shown in Figure 29. As predicted by the original OEM analysis, it is above the operating speed of the pump.

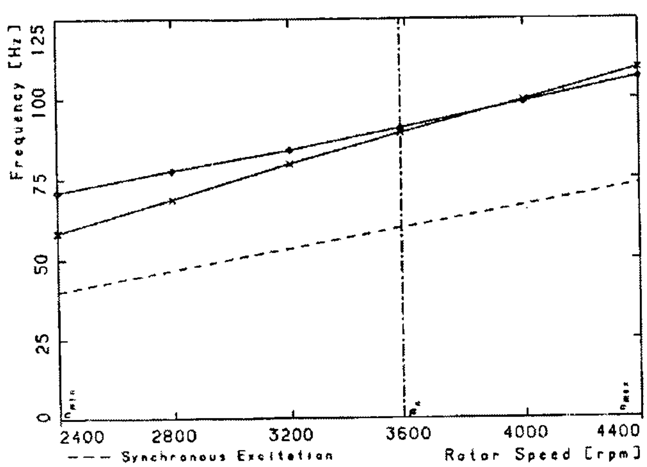

Figure 26. OEM Campbell Diagram.

The bushings and wear rings were modeled with a bulk flow model of Hirs' leakage equation (HSEAL, 1995; San Andres, 1991). As it would be expected, decreasing the clearance of the center and throttle bushings increased the stiffness and damping produced by these bushings. Figures 30 and 31 show the stiffness and damping coefficients for the center bushing with the original and reduced clearance. This has no effect on the first mode, and only raises the value of the second mode by less than 1 percent, though it had little effect on the stability of the rotor (Figure 32).

Changing the impeller diameter has very little effect on the wear ring coefficients, other than increasing the differential pressure across the wear rings, which tends to stiffen them. For this small of

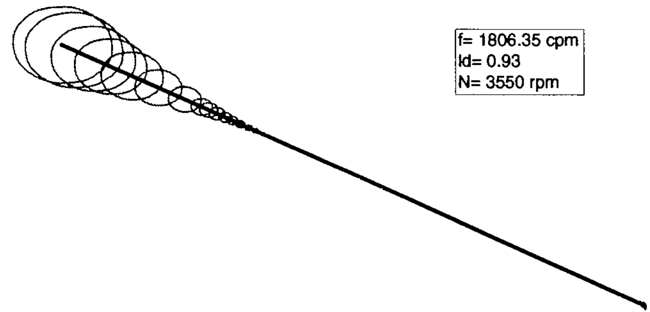

Figure 27. First Lateral Mode Shape (Original OEM Clearances).

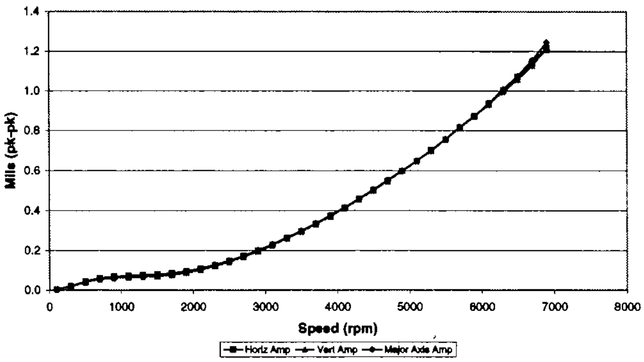

Figure 28. Forced Response Plot of DE Bearing.

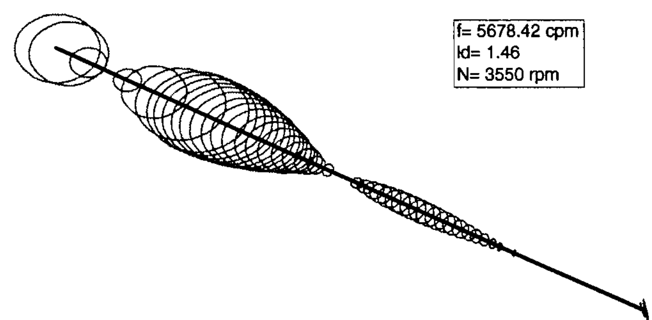

Figure 29. Second Lateral Mode Shape (Original OEM Clearances).

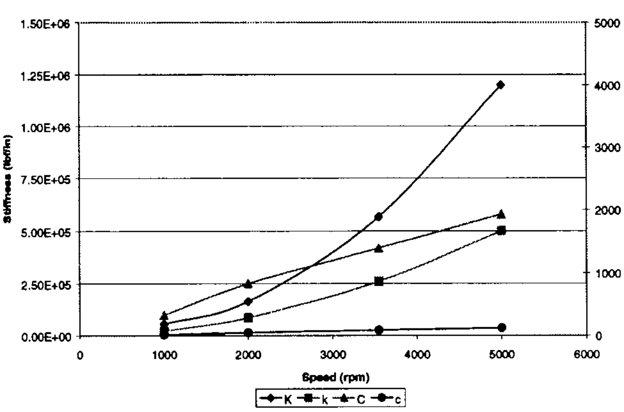

Figure 30. Stiffness and Damping Coefficients of Original Center Bushing.

an increase in discharge pressure, the difference in the seal coefficients is negligible. However, for obvious reasons, the impeller coefficients should change.

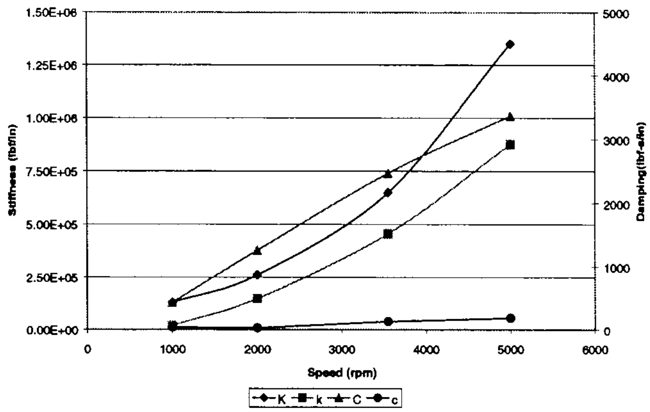

Figure 31. Stiffness and Damping Coefficients of Modified Center Bushing.

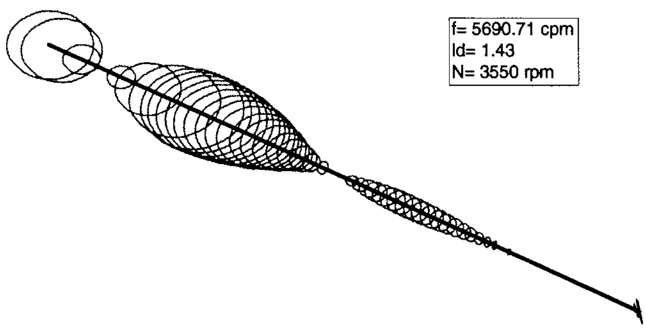

Figure 32. Second Lateral Mode Shape (Modified Clearances).

While there are many computer programs that predict bearing and annular seal coefficients, impeller coefficients are not as readily available. The impeller coefficients were calculated from the empirical data of both Jery, et al. (1985), and Bolleter, et al. (1984) (Table 1). Childs (1993) has shown that most impellers have coefficients somewhere between the two.

Table 1. Nondimensional Impeller Coefficients.

Coefficient	Impellers with large clearances Jery, et al. (1985)	Impellers with small clearances Bolleter, et al. (1984)
K	−2.5	−4.2
k	1.1	5.1
C	3.14	4.6
c	7.91	13.5
M	6.51	11.0
m	−0.58	4.0

These nondimensional coefficients were converted to their dimensional form for the impellers in the HDW charge pump and are shown in Table 2. As can be seen, for this application the magnitude of these coefficients is small in comparison to the bushing coefficients, which have an order of magnitude of 1×10^5.

Table 2. Dimensional Form of Impeller Coefficients, at Design Speed of 3550 RPM.

Coefficient	Impellers with large clearances Jery, et al. (1985)	Impellers with small clearances Bolleter, et al. (1984)
K	−1990.3	−3343.7
k	875.7	4060.2
C	6.7	9.9
c	16.9	28.9
M	0.03750	0.06337
m	−0.00334	0.02304

The original mode shapes shown in Figures 27 and 29 were calculated using the impeller coefficients of Jery, et al. (1985). Figures 33 and 34 show the first and second mode shapes with the reduced clearance throttle bushings and the small clearance impeller coefficients of Bolleter, et al. (1984) (Table 2). As can be seen, there is very little difference between the calculated modes.

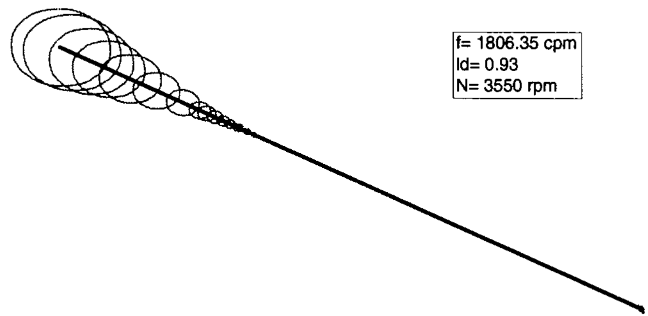

Figure 33. First Mode Shape with Impeller Coefficients of Bolleter, et al. (1987).

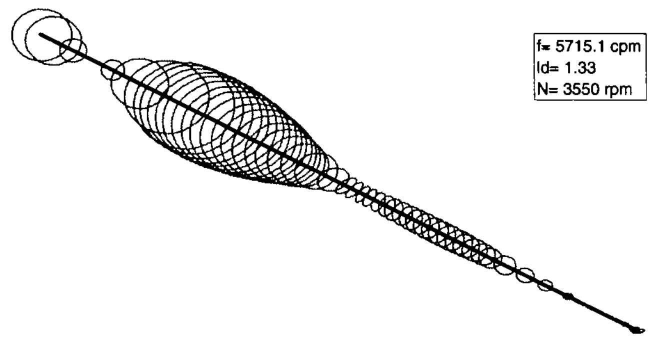

Figure 34. Second Mode Shape with Impeller Coefficients of Bolleter, et al. (1987).

RESULTS

The modified rotor and bushings were installed in the HDW charge pump in February of 1999. The performance was measured immediately after startup and was found to be above the predicted values (Figure 35). This was probably a result of improvements in efficiency caused by the reduced vane-to-volute clearance that was not taken into account. Since then, the performance has been checked several times and has shown no decrease. The overall vibration of the HDW charge pump has been less than 1.0 mil of shaft displacement since the modification. Figures 36 and 37 are shaft vibration spectra from before and after the modification.

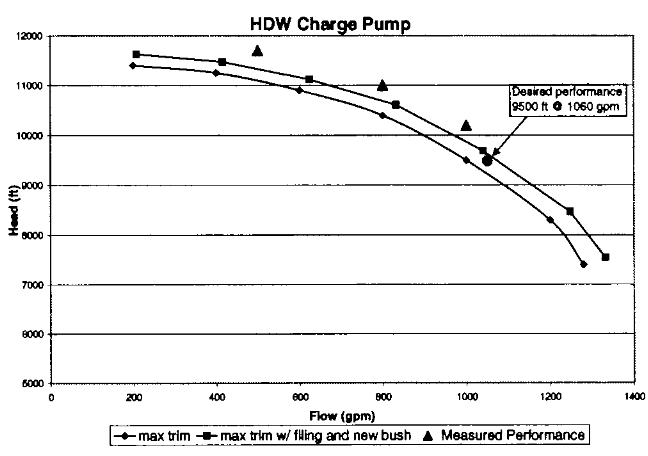

Figure 35. Predicted Performance Curve with Underfiling and Measured Performance.

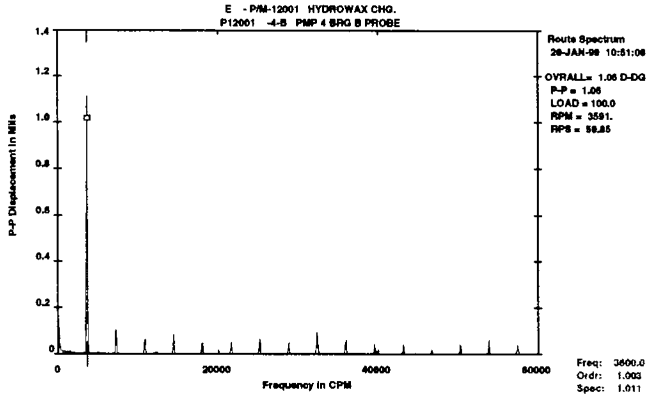

Figure 36. Shaft Vibration Before Upgrade.

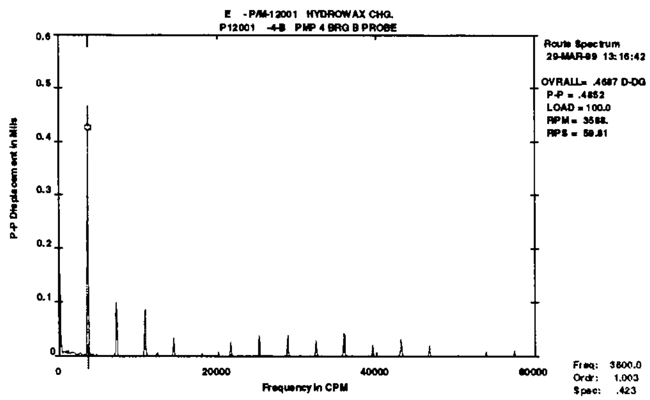

Figure 37. Shaft Vibration After Upgrade.

CONCLUSIONS

The use of dual seals (either pressurized or nonpressurized) does not automatically increase the reliability of pumps in heavy gas oil service. Heavy process streams that can collect in the seal pots may pose a serious problem for the secondary seal. Also, precaution should be taken in high surface velocity applications to ensure that the secondary seal will receive adequate lubrication. Likewise, if the axial length of the dual seal prevents installation of an anti-coking device, it can affect the reliability of the seal. The maximum speed rating of the seal should be considered when selecting rotating versus nonrotating bellows.

Increasing the impeller diameter beyond the API recommended 6 percent tip clearance should only be done with caution. Certain precautions such as underfiling impeller vanes and increasing the damping in supports should be done to prevent a vane pass vibration problem. However, it can be done successfully if the pump rotor is sufficiently stable.

NOMENCLATURE

C = Absolute fluid velocity vector, fps or damping coefficient in principal direction
D = Impeller diameter, ft
H = Fluid head, lbf-ft/lbm
K = Stiffness coefficient, principal direction
k = Stiffness coefficient, cross-coupled term
u = Impeller velocity vector, fps
w = Relative fluid velocity vector, fps
z = Number of impeller vanes

Symbols

β = Impeller vane angle, degrees
μ = Slip factor, nondim

Subscripts

1 = Impeller inlet conditions
2 = Impeller exit conditions
F = Filed conditions
m = Meridian component
u = Tangential component

REFERENCES

Bolleter, U., Frei, A., and Florjancic, D., 1984, "Predicting and Improving the Dynamic Behavior of Multistage High Performance Pumps," *Proceedings of the First International Pump Symposium*, Turbomachinery Laboratory, Texas A&M University, College Station, Texas, pp. 1-8.

Childs, D. W., 1993, *Turbomachinery Rotordynamics*, New York, New York: John Wiley & Sons.

HSEAL – A Computer Program for: Calculating Rotordynamic Coefficients and Leakage on Incompressible Flow Annular Seals, v. 2.2, 1995, Rotordynamics-Seal Research, Inc., North Highlands, California.

Jery, B., Brennen, C. E., Caughey, T. K., and Acosta, A. J., 1985, "Forces on Centrifugal Pump Impellers," *Proceedings of the Second International Pump Symposium*, Turbomachinery Laboratory, Texas A&M University, College Station, Texas, pp. 21-32.

Karassik, I. J., Krutzsch, W. C., Fraser, W. H., and Messina, J. P., Editors, 1986, *Pump Handbook*, Second Edition, New York, New York: McGraw-Hill, Inc.

Lebeck, A. O., 1991, *Principals and Design of Mechanical Face Seals*, New York, New York: John Wiley & Sons.

San Andres, L. A., October 1991, "Analysis of Variable Fluid Properties, Turbulent Annular Seals," ASME Journal of Tribology, *1113*, pp. 694-702.

BIBLIOGRAPHY

API, *Centrifugal Pumps for Refinery and Chemical Service*, Eighth Edition, American Petroleum Institute, Washington, D.C.

Corbo, M. A. and Malanoski, S. B., 1998, "Pump Rotordynamics Made Simple," *Proceedings of the Fifteenth International Pump Users Symposium*, Turbomachinery Laboratory, Texas A&M University, College Station, Texas, pp. 167-204.

Sulzer Pumps Ltd., 1998, *Sulzer Centrifugal Pump Handbook*, Second Edition, Oxford, United Kingdom: Elsevier Advanced Tech.

Valantas, R. A. and Bolleter, U., 1988, "Solutions to Abrasive Wear-Related Rotordynamic Instability Problems on Prudhoe Bay Injection Pumps," *Proceedings of the Fifth International Pump Users Symposium*, Turbomachinery Laboratory, Texas A&M University, College Station, Texas, pp. 3-10.

Vance, J., 1988, *Rotordynamics of Turbomachinery*, New York, New York: John Wiley & Sons.

Verhoeven, J. J., 1988, "Rotordynamic Considerations in the Design of High Speed, Multistage Centrifugal Pumps," *Proceedings of the Fifth International Pump Users Symposium*, Turbomachinery Laboratory, Texas A&M University, College Station, Texas, pp. 81-92.

ACKNOWLEDGEMENTS

The paper would not have been possible without the contributions of the following individuals: Sonia Bordelon of Conoco, David Lowe of Flowserve, Bert Flynn and Art Washburn of Sulzer Pumps, Dr. Alan Lebeck of MSTI, and Mark Corbo of No Bull Engineering.